Applications of neural networks to simulate soil-tool interaction and soil behavior

Z.X. ZHANG and R.L. KUSHWAHA

Department of Agricultural and Bioresource Engineering, University of Saskatchewan, 57 Campus Drive, Saskatoon, SK, Canada S7N 5A9. *Received 13 September 1998; accepted 14 May 1999.*

Zhang, Z.X. and Kushwaha, R.L. 1999. **Applications of neural networks to simulate soil-tool interaction and soil behavior**. Can. Agric. Eng. **41**:119-125. Principles of radial basis function (RBF) neural network and its application procedure have been described using simulation of (1) tool draft at high operating speed, (2) frozen soil strength behavior associated with factors such as confining pressure, strain rate, and soil temperature, and (3) soil freezing and thawing processes. In the first illustrative example, the relation between draft and operating speed, tool and soil types were established using a RBF network. In the second example the relationship between frozen soil strength and confining pressure, strain rate, soil dry density, and soil temperature were depicted. The final example was to predict soil temperature as a function of air temperature, elapsed time, and depth during soil freezing and thawing processes. These illustrative examples indicated that the RBF network is a powerful tool for simulating highly nonlinear systems that are difficult to describe using analytical methods.

Les principes de la fonction de base radiale (FBR) pour un réseau neuronal ainsi que sa procédure d'application ont été décrits en utilisant la simulation: d'un outil de traction à haute vitesse (1), des comportements des forces qui agissent dans les sols gelés associés avec des facteurs tel que la pression confinée, le taux de déformation et la température du sol(2), des processus de gel et de dégel des sols. Dans le premier exemple, la relation entre la traction et la vitesse d'opération ainsi qu'entre l'outil et le type de sol a été établie en utilisant un réseau FBR. Dans le second exemple, la relation entre les forces agissant dans les sols gelés, la pression confinée, le taux de déformation, la densité sèche du sol ainsi que sa température a pu être décrite. Dans le dernier exemple, l'on a pu prédire la température du sol en fonction de la température de l'air, le temps écoulé et la profondeur de gel durant le gel et le dégel. Ces exemples montrent que les réseaux neuronaux FBR sont un outil puissant pour la simulation de systèmes non linéaires complexes et difficiles à analyser avec des méthodes analytiques.

INTRODUCTION

The artificial neural network (ANN) has become a powerful tool for modeling a system for which we have an incomplete understanding of its governing laws or for a system for which the governing laws are too complex to be solved. A remarkable feature of neural networks is that they can learn from the relationship between input and output from experiments and that they are capable of generalizations based on the knowledge that has been gained.

Application of ANN to model geotechnical problems has been investigated by several researchers. Ghaboussi et al. (1991) used a back-propagation (BP) network (Rumelhart et al. 1986) to model soil stress-strain relations. Goh (1995) also applied a BP network to model cone penetration and to predict load capacity of driven piles. The BP network is very commonly used in neural network applications due to its simple learning algorithm, but how to determine the number of hidden layers and the number of hidden neurons for each layer in the BP network largely depends on one's experience.

By comparison, the radial basis function (RBF) neural network (Powell 1987; Moody and Darken 1989) has a high learning efficiency in training the network. The structure of a RBF network is one of self-organized characteristics, which allow for adaptive determination of the hidden neurons in the training network. Flood (1996) has demonstrated a method to simulate the partial differential equation of heat flow in soil using a RBF network.

The objective of this study was to demonstrate principles and applications of neural networks to model tillage draft at high operating speed, the relationship between frozen soil strength and the confining pressure, strain rate, and soil temperature, and to simulate the soil freezing and thawing processes.

RADIAL BASIS FUNCTION NEURAL NETWORKS

The radial basis function (RBF) was originally proposed for the purpose of multivarable interpolation (Powell 1987), i.e. given m different points x_i $i = 1, 2, \bullet\bullet\bullet, m$ in R^n and m numbers y_i $i = 1, 2, \bullet\bullet\bullet, m$, to find a function, φ, satisfying $F(x_i) = y_i$. One form of the function is chosen as:

$$F(x) = \sum_{i=1}^{m} \lambda_i \phi \| x - c_i \| \qquad x \in R^n \tag{1}$$

where:

λ_i = coefficients,

$\varphi\|x - c_i\|$ = radial basis function, a strictly positive radial symmetric function (kernel), and

c_i = center of kernel.

The application of the radial basis function can been determined from (Mulgrew 1996):

multi-quadratic:

$$\phi(x) = \sqrt{x^2 + \sigma^2}$$

inverse multi-quadratic:

$$\phi(x) = \frac{1}{\sqrt{x^2 + \sigma^2}}$$

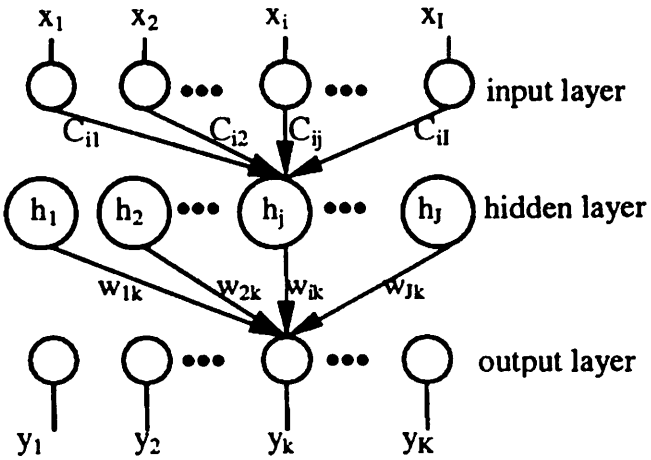

Fig. 1. RBF network architecture.

thin plate spline:

$$\phi(x) = \frac{x^2}{\sigma^2}\log\left(\frac{x}{\sigma}\right)$$

logistic function:

$$\phi(x) = \left[1 + \exp\left(\frac{x^2}{\sigma^2}\right) - \theta\right]^{-1}$$

Gaussian function:

$$\phi(x) = \exp\left(-\frac{x^2}{2\sigma^2}\right)$$

The RBF neural network has a feed-forward architecture, which consists of three layers: one input layer, one hidden layer, and one output layer, as shown in Fig. 1. Each neuron in the input layer (input neuron) is completely connected to all neurons in the hidden layer (hidden neuron) and hidden neurons and output neurons are also interconnected to each other by weight *w*. After an input neuron receives a signal, it transmits it to the hidden neurons. The output of information process of the hidden neurons has the form of a radial basis function. The Gaussian function (kernel) is the most widely employed as output of hidden neurons and can be expressed as:

$$h_j = \exp\left[-\frac{\|x - c_i\|^2}{2\sigma_j^2}\right] \qquad j = 1, 2, \cdots, J \qquad (2)$$

where:

h_j = output of hidden neuron *j*,
x = vector of input signal,
c_j = center of hidden neuron *j*,
σ_j = width of hidden neuron *j*, and
$\|\bullet\|$ = Euclidean distance.

The Gaussian function has a maximum output at the center and a rapid decay to zero as the input signals move away from the center of the receiving field. The signals that are at the center of the receiving field are called prototypes. Hidden neurons of a RBF network only respond to the input signals that are close to the prototype. The characteristic that neurons have such a locally tuned or selective response to the receiving field can be found in some nervous systems (Moody and Darken 1989). In the physical world, it is often assumed that nearby patterns are more likely to have the same classification than the distant ones and that similar things tend to have the same properties (Anderson 1995). Therefore, the Gaussian kernel in a RBF network has a response only to the similar classification of receiving patterns.

The neurons in the output layer have a linear output responding to the signals that are transmitted from the hidden neurons. For example, the output of neuron *k* in the output layer can be expressed as:

$$y_k = \sum_{j=1}^{J} w_{kj} h_j \qquad k = 1, 2, \cdots, K$$

where:

y_k = output of neuron *k* in output layer, and
w_{kj} = weight connected to hidden neuron *j* and output neuron *k*.

From the surface modeling interpretation, Eq. (3) can be interpreted as a hypersurface with the superposition of Gaussian bell-shaped surfaces. The shape of a hypersurface depends on the number of hidden neurons, the center c_j, width σ_j, and weight w_{kj}. The task of training the RBF network is to determine the number of hidden neurons and the value of the center, width, and weight based on a given learning sample of the relationship between input and output.

In training a RBF network, the number of hidden neurons is self-organized with the process of training. Specifically, at the beginning of training a RBF network, the number of hidden neurons is zero. The hidden neurons are added one by one with training until the output of the network is within a target precision. In training every hidden neuron, the center is assigned to the training input pattern where the maximum sum of squared error occurs. For this purpose, the k-mean clustering technique was employed (Moody and Darken 1989).

The width was set as a global constant in this study, i.e. the width of all hidden neurons has the same value. However, it was found that the capacity of the RBF network generalizations was closely dependent on the width. To illustrate this argument, take learning a unit circle as an example as shown in Fig. 2. The numbers (1 to 9) were used as the training pattern input to the RBF network and the coordinate corresponding to these points as output (Fig. 2a). The problem in this example was to map the numbers from 1 to 9 into a circle, i.e., 1 was mapped into the coordinate of (1,0), 2 into ($\sqrt{2}/2$, $\sqrt{2}/2$), 3 into (0,1), and so on. After the network was trained, the test pattern for input to the network was chosen from 1 to 9 with increment of 0.2 (i.e. 1, 1.2, 1.4, ..., 9). The output of the network was the coordinate corresponding to the input number. The capability of network generalization in the case of $\sigma = 0.3$, $\sigma = 0.5$, and $\sigma = 10$ is illustrated in Fig. 2b to Fig. 2d, where symbols were the trained points and curves were generalized by the network. The figures show that the generalized curve has a big error compared to the unit circle at $\sigma = 0.3$ (Fig 2b), but the curve is very close to the circle at $\sigma = 10$ (Fig.2d).

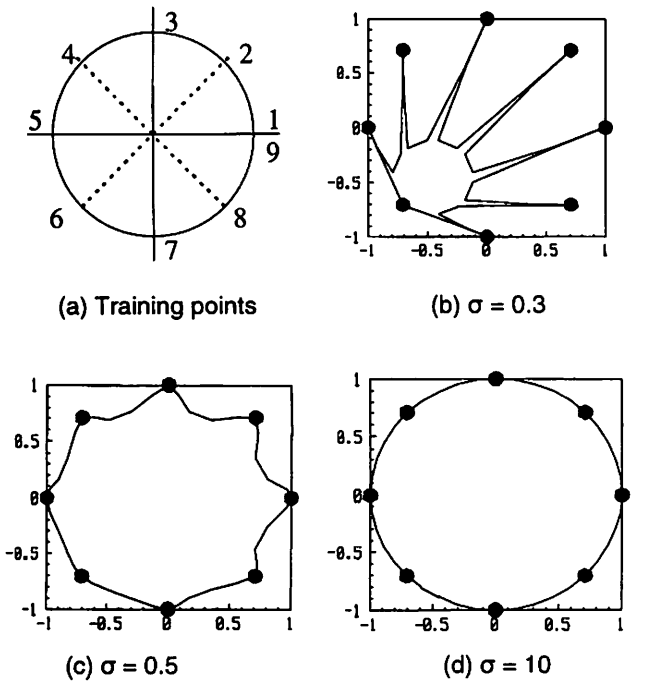

Fig. 2. Capacity of RBF generalization with different width.

SIMULATION OF DRAFT AT HIGH OPERATING SPEED

The tool draft is dependent upon operating speed. The mechanism that accounts for the draft increases with the increase in operating speed is associated with soil inertial effect, soil strength rate effect, and wave propagation effect. Consequently, the relationship between draft and operating speed exhibits a complex characteristic. For example, Fig. 3 shows experimental results of draft response to high operating speed given by Linke and Kushwaha (1992). The tests were conducted in three field sites, sandy soil (field 1), sandy stony soil (field 2), and clay soil (field 3) with five different narrow blades. The operating speed ranged from 5 km/h to 60 km/h. It was indicated that the characteristics of draft-speed relation varied greatly with tools and soil types. To obtain the relation of draft with operating speed, tools, and soil types using a RBF neural network, operating speed, tools, and soil types were used as input to the network and draft was used as the output of the network. The training pattern with N learning samples was constructed as:

$$\mathbf{P} = [P_1, P_2, \bullet\bullet\bullet, P_N] \qquad \mathbf{T} = [T_1, T_2, \bullet\bullet\bullet, T_N] \qquad (4)$$

where:

P, T = input and output pattern for training network, respectively,

P_i = $[V_i, B_{1i}, B_{2i}, B_{3i}, B_{4i}, B_{5i}, S_{1i}, S_{2i}, S_{3i}]'$ (i = 1, 2, •••, N),

P_i = ith learning sample input to network,

V_i = operating speed in the ith learning sample,

$B_{1i}, B_{2i}, \bullet\bullet\bullet, B_{5i}$ = narrow tools used in the ith learning sample,

S_{1i}, S_{2i}, S_{3i} = soil types used in the ith learning sample, and

F_i (i = 1, 2, •••, N) = draft corresponding to the ith learning sample.

Since soil and tool types must be quantified before they can be used for training the network, a simple strategy for quantifying of soil and tool type was used as 0 (zero) and 1 (one). Specifically, soil classification or tool type was set to one if it was selected in a learning sample, otherwise, it was set to zero. For instance, a learning sample for operating speed of 10 m/s, tool type 1 and soil type 2 was presented as P_i = [10 1 0 0 0 0 1 0 0]. In this way, a total of 166 learning samples were chosen for training the network. Experience indicated that the normalization of the input and target pattern, **P** and **T**, was helpful for the improvement of learning efficiency in training

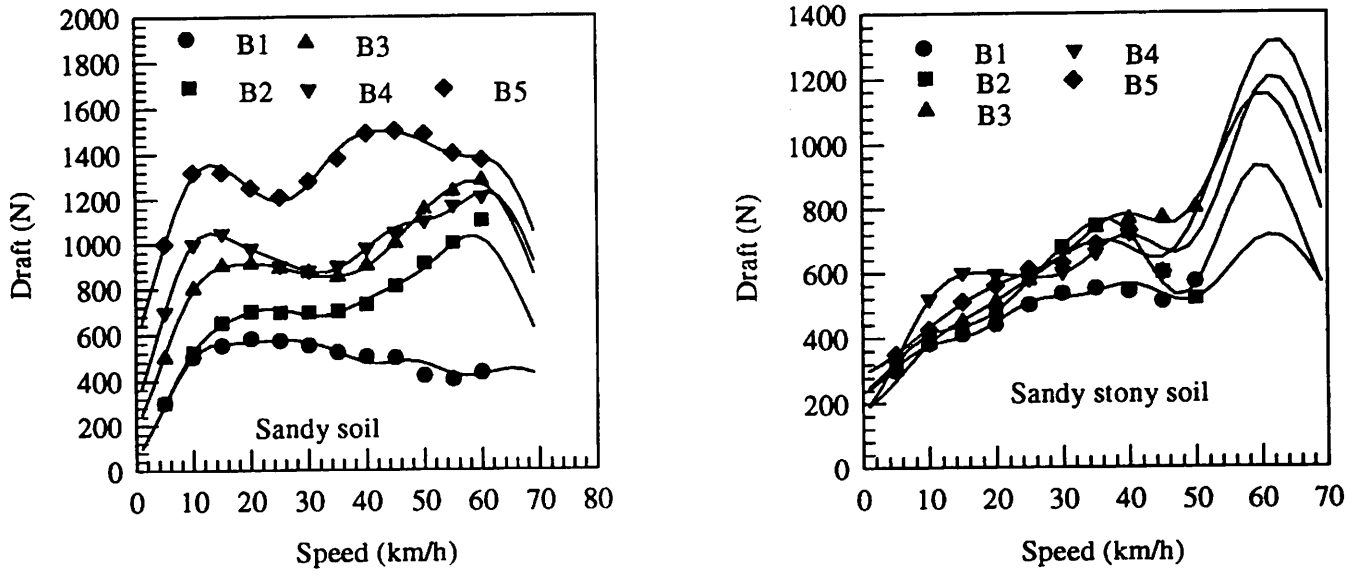

Fig. 3. Draft vs speed for sandy and sandy stony field.

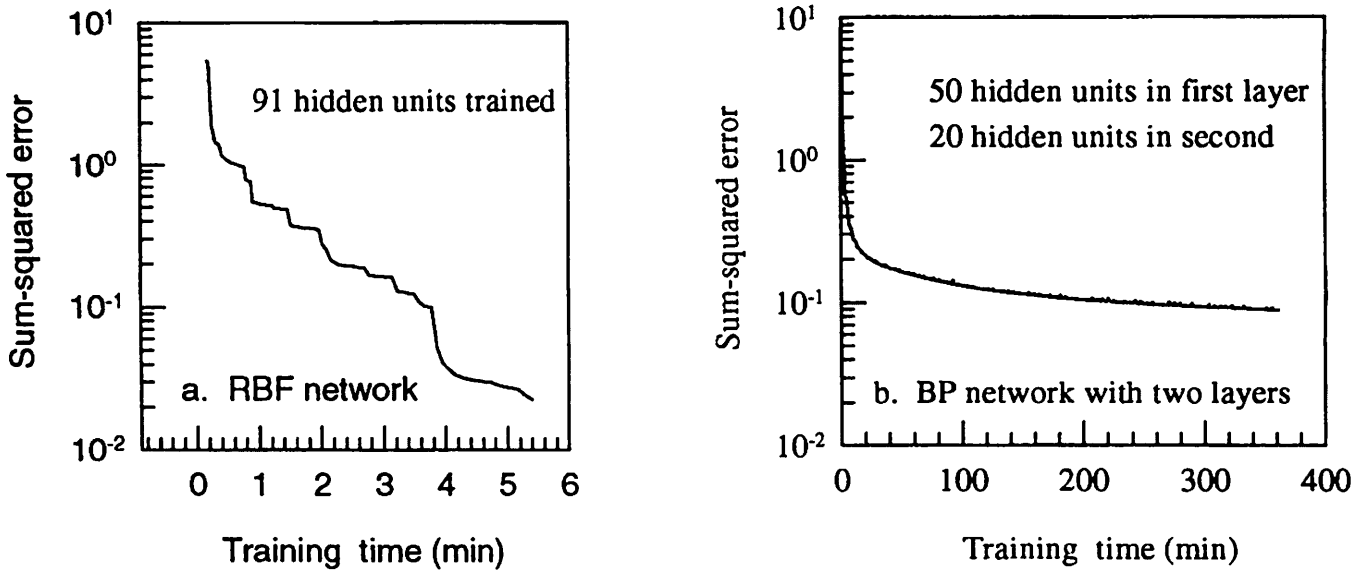

Fig. 4. Sum-squared-error vs the training time for RBF and BP networks.

a network. For this purpose, a transformation was carried out as:

$$V_i' = V_i / V_m, \qquad F_i' = F_i / F_m \tag{5}$$

where V_m, F_m = maximum value of operating speed and draft, respectively.

The process of training the network is illustrated in Fig. 4. After training the network, 91 hidden neurons were learned and it took 5.5 minutes for the given goal error (sum of squared error) of 0.02 (Fig. 4a). By comparison, for the same problem, the BP network had not reached the goal error (0.02) after learning for 361.45 minutes (Fig. 4b). This indicates that the RBF network has a higher learning efficiency than the BP network. To test the capability of generalization for the trained network, a test pattern was designed with the speed input from 1 km/h to 70 km/h with increment of 0.1 km/h. The results obtained from the network for various soils and tools are illustrated as continuous lines in Fig. 3. The figures show that the trained network yields a very good generalization in the sense of interpolation.

SIMULATION OF FROZEN SOIL STRENGTH

The strength of frozen soil is closely associated with temperature, strain rate (or loading time), and confining pressure, in addition to soil classification, soil density, and soil moisture. There is no well-established theory that can describe the behavior of frozen soil strength related to the change in these factors. Since limited data were available, only two simple examples were used to depict the behavior of frozen soil strength via neural network.

The relationship between the strength of frozen sand and confining pressure, soil density, and saturation is illustrated in Fig. 5, where the solid symbols are the experimental results. The mechanical and thermal effect on ice weakening could account for such a property of the frozen soil strength (Zhang et al. 1993). To simulate the effect of soil dry density on the relationship between frozen soil strength and confining pressure with the RBF network, dry density and confining pressure were used as the network inputs and frozen soil strength as output. In this example, a total of 40 learning samples were built to construct the training pattern, that is:

$$\mathbf{P} = [\mathbf{P}_1 \ \mathbf{P}_2 \ \cdots \ \mathbf{P}_{40}] \qquad \mathbf{T} = [q_1 \ q_2 \ \cdots \ q_{40}] \tag{5}$$

where:

- $\mathbf{P}$ = input training pattern,
- P_i = $[\gamma_i \ \ p_i]'$ $(i = 1, 2, \cdots, 40)$
- γ_i, p_i = soil dry density and confining pressure for the ith learning sample,
- $\mathbf{T}$ = target output of training pattern,
- q_i $(i = 1, 2, \cdots, 40)$ = maximum deviatoric stress of frozen sand corresponding to the ith input learning sample.

After the network was trained, the network predictions as a function of confining pressure for different dry densities are illustrated as solid curves in Fig. 5. The predicted curves at dry density of 1700 kg/m^3 and 1800 kg/m^3 display a reasonable tendency with respect to the curves which have good agreement with the measured data at soil densities of 1600 kg/m^3 and 1900 kg/m^3.

Similarly, the results of a RBF network to model frozen silt strength (Zhu and Carbee 1987) with the change in strain rate and temperature are given in Fig. 6. In this example, the strain rate and temperature were input to the network and the compressive strength of frozen silt as output. The soil temperatures at -1°C, -5°C, and -10°C are chosen as learning samples for the training network, as illustrated by solid symbols in Fig. 6. The training pattern is given as:

$$\mathbf{P} = [\mathbf{P}_1 \ \mathbf{P}_2 \ \cdots \ \mathbf{P}_{70}] \qquad \mathbf{T} = [\sigma_1 \ \sigma_2 \ \cdots \ \sigma_{70}] \tag{6}$$

where:

P_i = $[\theta_i \ \dot{\varepsilon}_i]^T$ $(1 = 1, 2, \cdots, 70)$,

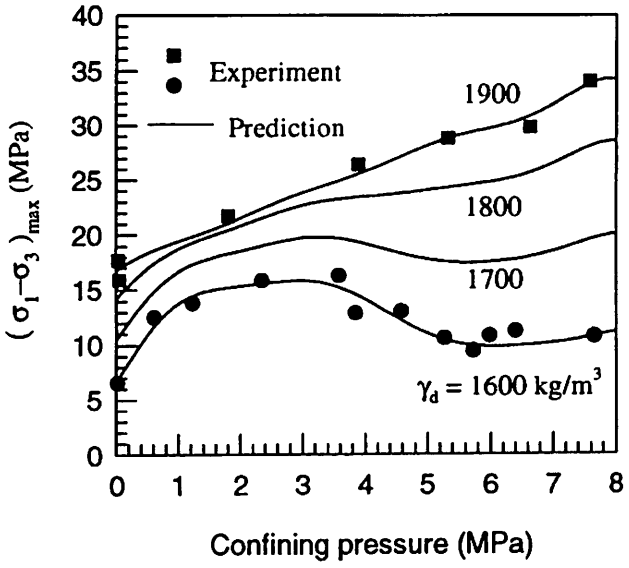

Fig. 5. Frozen sand strength vs confining pressure. Experimental data from Zhang et al. (1993).

θ_i, $\dot{\varepsilon}_i$ = soil temperature and strain rate for the ith learning sample,

σ_i (1 = 1, 2, •••, 70) = uniaxial compressive strength of frozen silt corresponding to the ith learning sample.

After the training network was completed for the target of squared-sum-error of 0.02, only 18 hidden neurons were trained. The trained network made satisfactory generalizations for the new input pattern in which strain rate changed from 10^{-7} to 1 s^{-1} and temperature from -0.5 °C to -10 °C (Fig. 6). The solid symbols are experimental data that were used in the training network, the blank symbols are the data that were not used in training, and the curves are the results from the network simulation.

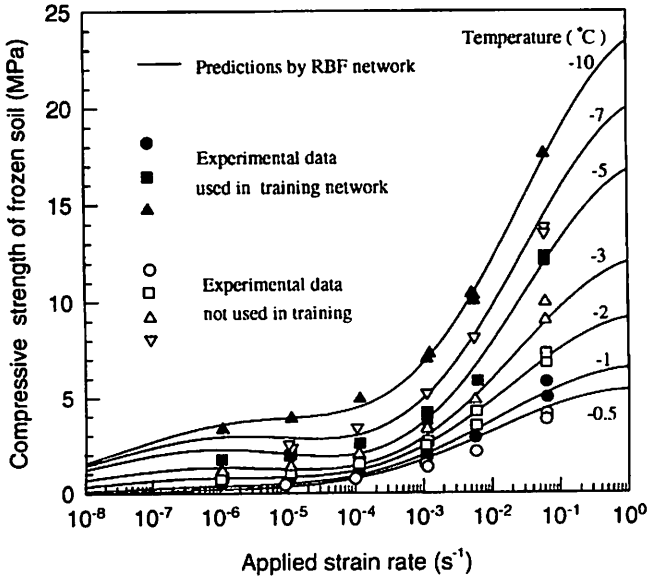

Fig. 6. Strain rate behavior of frozen silt strength. Experimental data from Zhu and Carbee (1987).

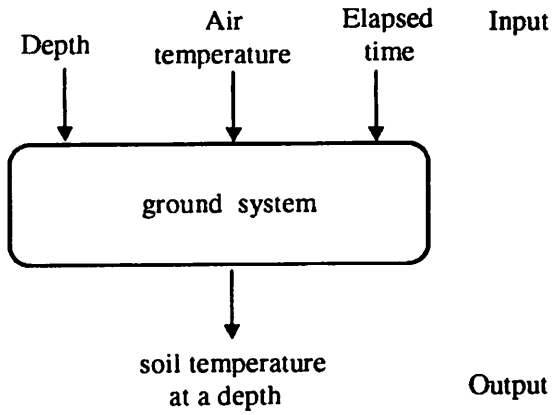

Fig. 7. Schematic of the system of soil freezing and thawing.

SIMULATION OF GROUND TEMPERATURE DURING FREEZING AND THAWING

Theoretically, the distribution of ground temperature can be computed using numerical calculations such as finite element or finite difference methods, based on soil and water conduction. However, it is difficult to acquire complete information on the physical and thermal properties related to the radiation of heat from ground cover and flow of the heat through soil and water. From system analysis and an engineering view point, the interests in modeling ground freezing and thawing processes could be described by macro-observational factors that can be easily measured, such as air temperature. For a given field, the soil temperature is associated with air temperature, elapsed time, and the depth below ground surface. It could be simulated with a black or gray box, as shown in Fig. 7.

The relationship between the system input and output in Fig. 7 can be learned from the measured data in training a network. Based on the experience that has been gained, the trained network will make a reasonable generalization for the new input information. To illustrate this argument, an experiment on soil freezing and thawing process was conducted in the laboratory. The measured air temperature in a cold cabinet and soil temperature at different depths is shown in Fig. 8. Twenty-six data of air temperature and elapsed time were extracted from these measured data to train the network. The value of depth, air temperature, and time are given in Table I.

From these values, a training pattern, which was composed of 156 learning samples, was constructed such that:

$$\mathbf{P} = [\mathbf{P}_1 \ \mathbf{P}_2 \ \bullet\bullet\bullet \ \mathbf{P}_{156}] \qquad \mathbf{T} = [\theta_{s1} \ \theta_{s2} \ \bullet\bullet\bullet \ \theta_{156}] \qquad (7)$$

where:

$\mathbf{P}$, $\mathbf{T}$ = input and target output of training pattern, respectively,

P_i = $[d_i \ \theta_{ai} \ t_i]'$ (i = 1, 2, ••• 156)

d_i, θ_{ai}, t_i = depth, air temperature, and elapsed time for ith learning sample, and

θ_{si} = soil temperature corresponding to the ith input learning sample.

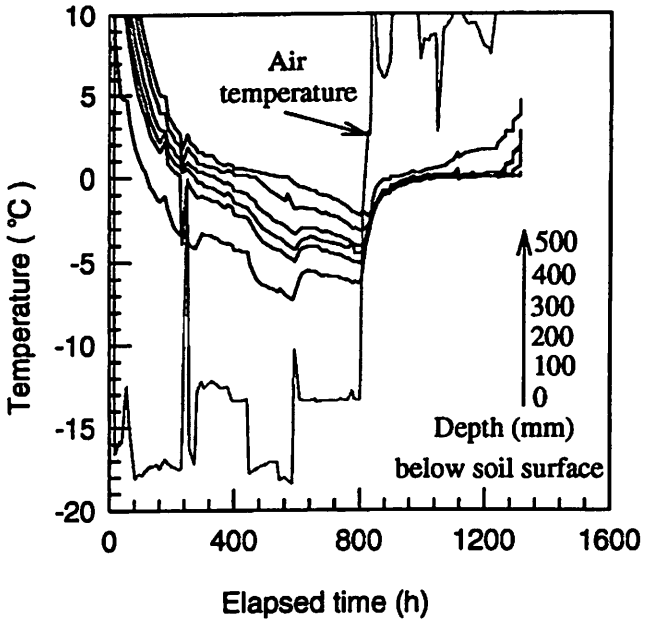

Fig. 8. Air and soil temperature vs elapsed time.

According to the given training pattern, a total of 50 hidden neurons was trained with $\theta = 3$ before a target squared-sum-error of 0.02 had been reached. To test the capability of generalizations for the trained network, a test input pattern was designed in which the depth changed from 0 to 500 mm with

Table I. The value of depth, air temperature, and elapsed time for training pattern.

Depth (mm)					
0	100	200	300	400	500
Air temperature (°C)					
20.5	-12.5	-17.9	-17.2	-17.4	-0.1
-12.2	-12.4	-13.4	-13.3	-17.3	-17.1
-18.4	-13.4	-13.4	-13.4	-12.8	2.7
13.6	6.7	9.2	11.7	7.2	8.7
9.6	10.5				
Elapsed time (h)					
11.3	55.5	106.0	153.5	203.0	248.8
296.0	345.0	394.0	441.6	489.8	537.8
585.0	634.5	681.5	731.0	777.0	825.2
838.1	856.2	898.3	945.0	992.5	1041
1088	1115				

Table II. The value of depth, air temperature, and elapsed time for testing pattern.

Depth (mm)					
0	10	20	30	...	500
Air temperature (°C)					
-17.3	-16.9	-17.6	-12.3	-13.4	-17.6
-18.0	-13.3	-13.4	13.3	6.1	9.1
Elapsed time (h)					
130.0	178.0	226.0	320.1	417.7	465.7
561.3	657.0	753.5	837.7	880.5	1065

increments of 10 mm and the value of air temperature and the elapsed time are given in Table II. The trained network predications as a function of depth at different elapsed times are shown in Fig.9, where the symbols indicate experimental data and curves are the predicted values. It can be seen from the figures that the trained network yields a good generalization for the given test pattern, except for a few cases. For example, at time 178 h during the period of soil freezing and 880 h during soil thawing, the network predictions deviated, to some degree, from the measured value.

CONCLUSIONS

1. The RBF network is an effective tool for recognition of a system pattern whose governing law has not been fully understood. The model established by a neural network is equivalent to an empirical model. However, an ANN simulation can establish a highly nonlinear relation to multivariable inputs.
2. The illustrated solutions, modeling draft at high operating speed, variation of frozen soil behavior with confining pressure, strain rate, soil dry density, and temperature, and predication of the temperature of freezing and thawing soil with air temperatures, and elapsed time, are formidable problems using analytic methods. However, the RBF network demonstrated very satisfactory generalizations in the sense of interpolation related to these problems.
3. Finally, it must be noted that because of the locally tuned feature of Gaussian neuron response, an RBF network is weak in extrapolation. To improve this shortcoming, the domain of input space should be chosen as large as possible.

ACKNOWLEDGMENTS

The authors gratefully thank the financial support from the Natural Science and Engineering Research Council of Canada.

REFERENCES

Anderson, J.A. 1995. *An introduction to Neural Networks.* Cambridge MA: MIT Press.

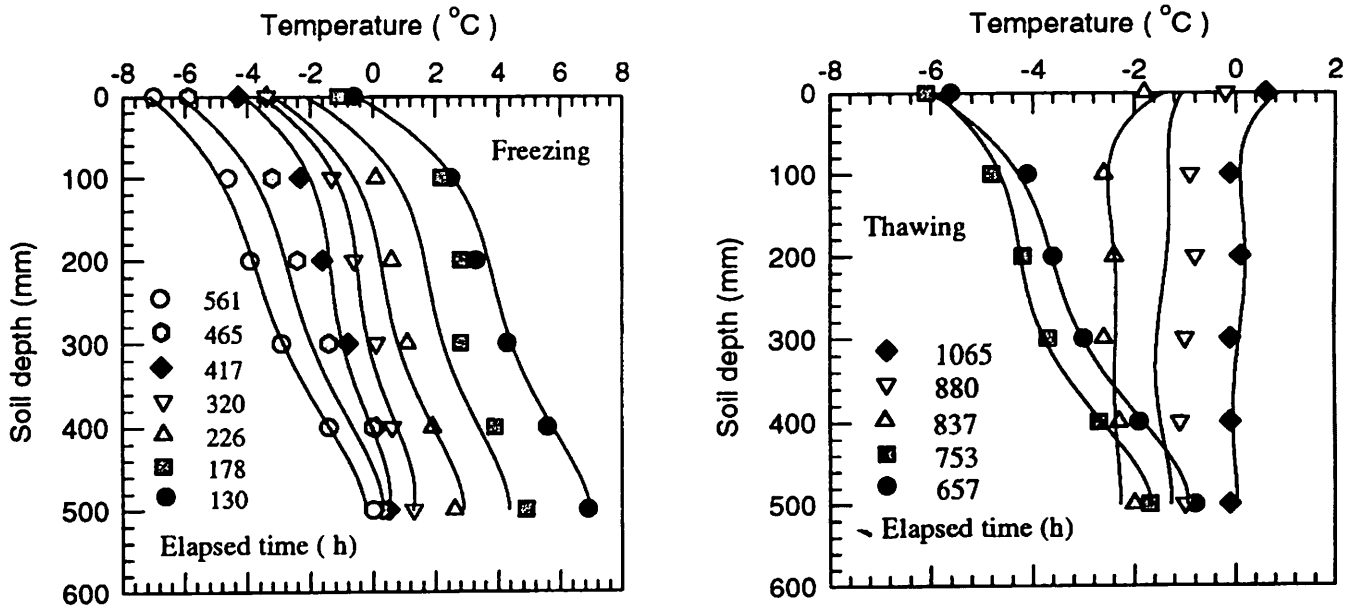

Fig. 9. Soil temperature vs depth during freezing and thawing (symbols - experiments; curves - predictions).

Flood, I. 1996. Simulating the behavior of poorly understoodcontinua using neural networks. *Artificial Intelligence for Engineering Design, Analysis and Manufacturing* 10: 391-400.

Ghaboussi, J., J.H. Garrett Jr, and X. Wu. 1991. Knowledge-based modeling of material behavior with neural networks. *Journal of Engineering Mechanics* 117(1):132-153.

Goh, A.T.C. 1995. Back-propagation neural networks for modeling complex systems. *Artificial Intelligence in Engineering* 9:143-151.

Linke, C. and R.L. Kushwaha. 1992. High speed evaluation of draft with a vertical blade. ASAE Paper No: 921019. St. Joseph, MI:ASAE

Moody, J. and C.J. Darken. 1989. Fast learning in networks of locally-tuned processing units. *Neural Computation* 1: 281-294.

Mulgrew, B. 1996. Applying radial basis functions. *IEEE Signal Process Magazine* 13(2): 50-65.

Powell, M.J.D. 1987. Radial basis functions for multivariable interpolation: A review. In *Algorithms for Approximation*, eds. J.C. Mason and M.G. Cox, 143-167. Oxford, NY: Oxford University Press.

Rumelhart, D.E., G.E. Hinton and R.J. Williams. 1986. Learning internal representations by error propagation. *Parallel Distributed Processing: Explorations in the Microstructures of Cognition*, Vol. I, eds. D.E. Rumelhart and J.L. McCleland, 318-362. Cambridge, MA: MIT Press.

Zhang, Z.X., Q. Yu, Z. Xen and H. Lu. 1993. Instantaneous-state deformation and strength of frozen soil. In *Proceedings of the Sixth International Conference on Permafrost*, Beijing, China, 5-9 July, 1993. Vol. 1: 797-802.

Zhu, Y. and D.L. Carbee. 1987. Creep and strength behaviors of frozen silt in uniaxial compression. CRREL Report 87-10. Hanover, NH: U.S. Army Cold Regions Research and Engineering Laboratory.